Unique Gold Nanoparticle Aggregates as a Highly Active Surface-Enhanced Raman Scattering Substrate

Adam M. Schwartzberg,[†,‡] Christian D. Grant,[†,§] Abraham Wolcott,[†] Chad E. Talley,[‡] Thomas R. Huser,[‡] Roberto Bogomolni,[†] and Jin Z. Zhang*[,†]

Department of Chemistry and Biochemistry, University of California, Santa Cruz, California 95064, and Department of Chemistry and Materials Science, Lawrence Livermore National Laboratory, Livermore, California 94550

Received: April 8, 2004; In Final Form: September 24, 2004

A unique gold nanoparticle aggregate (GNA) system has been shown to be an excellent substrate for surface-enhanced Raman scattering (SERS) applications. Rhodamine 6G (R6G), a common molecule used for testing SERS activity on silver, but generally difficult to detect on gold substrates, has been found to readily bind to the GNA and exhibit strong SERS activity due to the unique surface chemistry afforded by sulfur species on the surface. This GNA system has yielded a large SERS enhancement of 10^7-10^9 in bulk solution for R6G, on par with or greater than any previously reported gold SERS substrate. SERS activity has also been successfully demonstrated for several biological molecules including adenine, L-cysteine, L-lysine, and L-histidine for the first time on a gold SERS substrate, showing the potential of this GNA as a convenient and powerful SERS substrate for biomolecular detection. In addition, the SERS spectrum of R6G on single aggregates has been measured. We have shown that the special surface properties of the GNA, in conjunction with strong near-IR absorption, make it useful for SERS analysis of a wide variety of molecules.

Introduction

With the discovery of surface-enhanced Raman scattering (SERS), the potential for trace molecular detection using Raman scattering (RS) grew exponentially.[1−3] Previously RS had, to a large extent, been used exclusively for molecular structure interrogations.[4−6] An intrinsically small RS signal significantly limited its practical application. SERS possesses the molecular specificity of Raman scattering with greatly increased signal, making it ideal for many applications, from trace chemical detection of biomolecules and explosives[7−10] to structural interrogations of living cells.[11]

The ability to induce SERS is dependent on two key factors: resonant surface plasmon excitation of a metal substrate and close proximity of analyte molecules to the metal substrate surface. Surface plasmons are the result of the collective excitation of conduction band electrons near coinage metal surfaces, namely, gold and silver. When a surface plasmon is excited, an enhanced evanescent electromagnetic (EM) field is created at the metal surface. Calculations have shown that at dislocations or sharp discontinuities on a metal surface the EM field will be greatly enhanced.[12,13] Therefore, molecules in close proximity to the surface will experience a much larger EM field than if they were directly illuminated with light. The enhanced EM field decays exponentially from the surface and will induce strong RS of molecules within 0−4 nm of the surface.[14] Further discussion of the SERS mechanism is left to the many excellent review articles on this subject.[15−18]

* Author to whom correspondence should be addressed. E-mail: zhang@chemistry.ucsc.edu. Phone: (831) 459-3776. Fax: (831) 459-2935.

† Department of Chemistry and Biochemistry, University of California.

‡ Department of Chemistry and Materials Science, Lawrence Livermore National Laboratory.

§ Present address: Deptartment of Chemistry and Chemical Biology, Rutgers, Piscataway, NJ 08854.

Significant SERS enhancement is often present at the junction of two or more silver nanoparticles as shown recently by Brus and co-workers.[19] Little enhancement was observed for single nanoparticles in this study; however, aggregates with multiple particles yielded large enhancements due to what is believed to be the enormous EM field at junction sites. As two metal nanoparticles are brought together to form aggregates, their transition dipoles couple to each other. The enhanced fields of each particle begin to coherently interfere at the junction site between the particles. Calculations by Xu et al. have shown that electromagnetic enhancements of 10^{10} are present between two nanospheres separated by 1 nm.[20] These results suggest that aggregates are better substrates for SERS applications than individual nanoparticles because large enhancements can be achieved at particle junctions of aggregates.[21] In addition to the works by Brus and Xu, several studies have shown that intentional aggregation of gold and silver nanoparticles significantly increases the observed SERS enhancement.[22−27]

In addition to enhancing SERS activity of a substrate, aggregation of gold nanoparticles induces plasmon resonances in the near-IR (NIR) region. NIR absorption is highly desirable for many SERS applications, perhaps most notably are in vivo biological studies. Because tissues have an absorption minimum in the NIR, SERS of these materials can best be performed in this spectral region; however, a substrate with NIR absorption is required. Few substrates utilized have been capable of this; however, aggregated gold nanoparticles have strong NIR absorption.[28] The development of a SERS substrate such as this is potentially important for detecting biomolecules such as glucose noninvasively, necessary for many biomedical applications.[7] Not only is there a strong NIR absorption in aggregated gold nanoparticles, but this absorption is tunable by varying particle size and shape.

10.1021/jp048430p CCC: $27.50
Published on Web 11/17/2004

Because excitation must be on resonance with a maximum number of particles to achieve the largest enhancement possible, the ability to tune the NIR absorption of a SERS substrate is of the utmost importance. The nature of the surface plasmon absorption is entirely dependent on the metal used and the shape of the structure. With a change in the structure, it is possible to shift the surface plasmon of a metal nanostructure. A spherical nanoparticle of silver, for example, will show a single absorption band near 400 nm; however, if this particle is elongated into a nanorod, then a second absorption band between 500 and 800 nm will appear depending on length.[29] Similarly, in metal nanoshells,[30] aggregated nanoparticles,[31,32] and nonspherical nanoparticles,[33−36] new resonances are introduced leading to a variety of extended plasmon bands. For instance, three spherical particles closely interacting in a linear geometry will have two absorptions similar to a rod shaped particle of the same aspect ratio.[37] However, the same particles in a triangular geometry will have more than two resonances.[31] Therefore, with a change in the structure of the nanoshell, nanorod, or aggregate it is possible to effectively tune the position of the plasmon absorption band. This is ideal for SERS as the substrate is tuned to the desired excitation, not vice versa. Aggregates,[23] nanorods,[24,38] and metal shells[39−42] have been utilized for SERS studies; however, although it is possible to tune the absorption of these structures, aggregates have the advantage of greater enhancements due to intraparticle juncitons.

Although aggregates of nanoparticles may lead to the largest SERS enhancements, if the surface is not amicable to the target molecule, then SERS will not be possible. Surface chemistry of the substrate is critical for SERS because the analyte molecule must be within 0−4 nm of the substrate surface for the electromagnetic field to have an affect. Effectively, the molecule must bind to the metal surface to achieve SERS enhancement, a nontrivial problem for many molecules. For example, rhodamine 6G (R6G), a common dye used in colloidal silver SERS studies, generally does not adsorb to gold surfaces. Such binding selectivity makes engineering a generic SERS substrate challenging. An example of an ideal SERS substrate might be an aggregated nanoparticle system with strong and tunable NIR absorption and surface properties suitable for binding a variety of chemical and biological analytes. This is the first step to the development of a general analytical technique based on SERS that offers a unique combination of extremely high sensitivity and molecular specificity.

We have recently found that the broad near-IR absorption band of a unique gold aggregate system is inhomogeneously broadened due to different sized/shaped aggregates, based on oscillations observed in femtosecond transient absorption and persistent spectral hole-burning experiments.[43] The persistent hole-burning experiment in particular suggests that it may be possible to optically narrow the size/shape distribution of the aggregates for applications such as SERS. This aggregate system has been demonstrated to be SERS active in an early preliminary study.[44]

In this paper, we report a detailed study of the SERS activity of this gold nanoparticle aggregate (GNA) system that has unique surface properties and desired near-IR absorption for SERS applications. With R6G, an ensemble averaged Raman enhancement of approximately 10^7-10^9 has been estimated. The strong NIR absorption band, which is tunable between 600 and 1000 nm, is ideal for biological and physiological studies. NIR Raman also avoids resonance absorption of common biological molecules thereby reducing unwanted background fluorescence. Surface sulfur species allow the easy binding and detection of a variety of molecules, ranging from R6G to several biological molecules never before reported on gold SERS substrates. These molecules have been used to demonstrate the feasibility and versatility of this SERS substrate. The uniquely strong binding character is thought to be due to the high binding affinity of many molecules to the sulfur species on the surface of the GNAs.[45]

Experimental Section

The synthesis of the gold nanoparticle aggregates has been reported previously.[43,46] Briefly, 500 μL of a 0.02 M $HAuCl_4$ stock solution was diluted to 5×10^{-4} M with Milli-Q water in glassware cleaned in aqua regia and rinsed with Milli-Q water to avoid contamination. To this, 40−60 μL of a 0.1 M solution of Na_2S aged 2−3 months was added. After approximately 60−120 min, the color changed from a straw yellow to deep purple with the extended plasmon band (EPB) growing between 600 and 1000 nm, indicating reaction completion. The aggregate formation is signified by strong NIR absorption at wavelengths longer than 600 nm. Recent work in our lab has revealed that as the reaction progresses the aggregate structure changes from globular to linear as the EPB shifts from red to blue.[47] The aggregates are stable for weeks or months. After several days some aggregates do settle but can be dispersed easily with mixing. Absorption measurements were performed on a HP 89532A spectrometer with 2 nm resolution. Raman experiments were performed on a Nicolet Almega dispersive Raman spectrometer with excitation at 785 nm, 20 mW of power, and an integration time of 5 s averaged over 40 scans.

Samples for single particle experiments were prepared by immobilizing the GNAs on glass coverslips with trimethoxy-[3-(methylamino)propyl]silane (APS). Coverslips were cleaned prior to the silanization step by sonication in 2% solution of Hellmanex, followed by 18 MΩ water. They were then submerged in 5 mM aqueous solution of APS to deposit the tethering molecules. After 1−2 min, the coverslips were rinsed with water and dried under nitrogen, and 40 μL of the aggregate solution was placed on one surface. After several seconds exposed to the solution, it was blown dry with nitrogen.

Single particle experiments were performed on a custom designed confocal microscope built onto an inverted fluorescence microscope (Zeiss, Axiovert 100). A helium−neon laser (633 nm, Melles Griot) was coupled into the back port of the microscope and directed into a high numerical aperture objective (Zeiss Apochromat 100X, 1.4NA) that focused the light onto the sample surface. The sample was then raster scanned across the focused laser to generate an image using a commercially available piezoelectric scanner (Physik Instrumente) and control electronics (Digital Instruments). The Raman scattered light was collected with the same objective used for excitation and focused onto a confocal aperture. The Rayleigh scattered light was then removed using a holographic notch filter (Kaiser Optical), and the remaining Raman scattered light was focused onto an avalanche photodiode (EG&G). Once a nanoparticle aggregate was located, it was centered on the focused laser, and the Raman scattering was directed into a spectrograph (Acton Instruments), which dispersed the light onto a liquid nitrogen cooled CCD camera (Princeton Instruments). Typically six spectra (30 s) were averaged.

Results and Discussion

Figure 1 shows a typical electronic absorption spectrum of the gold nanoparticle aggregates. Two plasmon bands are present, corresponding to a transverse plasmon band (530 nm)

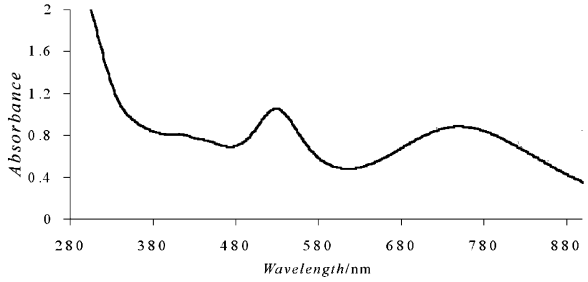

Figure 1. Representative UV−vis spectrum of gold nanoparticle aggregates. The two absorption bands correspond to transverse (530 nm) and extended plasmon bands (peaked around 760 nm).

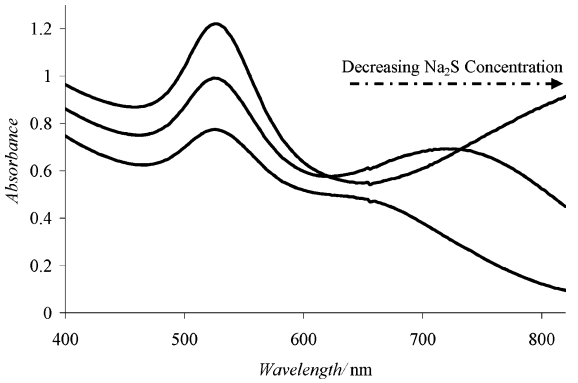

Figure 2. UV−vis absorption spectra of GNAs synthesized with varying concentrations of sodium sulfide. Initial Na_2S concentrations range from 0.8×10^{-4} M to 1.2×10^{-4} M red shifting with a decrease in this concentration.

and an extended plasmon band (EPB) (780 nm). Spherical gold particles will show only the transverse plasmon band due to their totally symmetric geometry.[28,31,48] Throughout the reaction, aggregates, not spherical particles, are formed as evidenced by the growth of the EPB indicating strong interparticle interactions. Previous work has shown that particle−particle separation is small, bound together by sulfur species on the nanoparticle surface.[45,49] Although similar absorption characteristics are observed in core/shell and nanorod structures, it was shown previously that the spectral characteristics here are due to strong particle−particle interation.[43,45,47,49] Interparticle distance is an important factor for SERS studies due to its direct correlation to electromagnetic enhancement. Xu et al. have reported that for two 90 nm nanoparticles, decreasing the spacing from 5.5 to 1 nm increases the theoretical enhancement by 4 orders of magnitude.[20] Particles such as these will have greater enhancements than other, weakly interacting systems with less intense EPBs.

With slight variation in reagent concentration, it is possible to shift the maximum of the EPB substantially. At standard sodium sulfide concentrations (0.1 mM), the absorption maximum will lie at approximately 780 nm. With an increase in the initial sodium sulfide concentration, the EPB will blue shift, and at lower concentrations it will shift to the red (Figure 2). Three main parameters affect the EPB position: aggregate size, shape, and individual particle size.[31] Altering any of these factors or combinations thereof will result in drastic changes in peak intensity and position. Generally, as GNAs grow larger, the EPB will red shift. However, aggregate shape also plays an important role in band position.[37] Reagent concentration undoubtedly affects not only shape but also size of both the individual nanoparticles and their aggregates, making an experimental distinction between size and shape difficult. The width of the

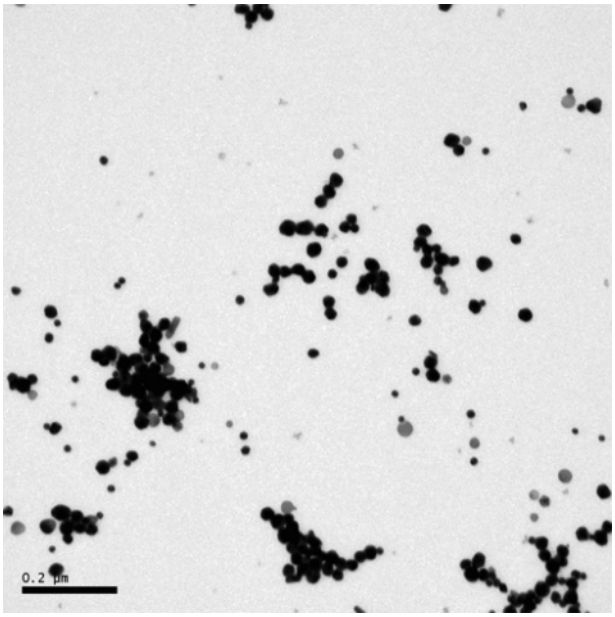

Figure 3. Representative TEM of gold nanoparticle aggregates showing strong interparticle interaction and a variety of aggregate sizes and shapes.

EPB, however, is simply dependent on the polydispersity of the size and shape of the aggregates.[32,43,50,51]

Because of the random nature of aggregate formation, the GNAs synthesized have a broad distribution of sizes and shapes. Each aggregate with a particular size and shape will have a unique EPB in terms of bandwidth and peak position. However, in an ensemble averaged solution, these bands will combine to form one strong, inhomogeneously broadened band.[32,43,50,51] This variety of sizes and shapes is apparent in the transmission electron microscopy (TEM) image in Figure 3. Figure 3 is a representative sampling of many different images and samples. The average particle size is on the order of ∼20 nm, with the particles making up aggregates, from small to large of many different structures. Each aggregate should have a different EPB depending on its size and shape.[31,32,43,50,51] Because the broad NIR EPB is composed of many narrower absorption bands, upon 785 nm excitation as used in the SERS experiments, only a subset of the aggregates will be on resonance and absorb this incident light. The percentage of aggregates being excited can be maximized by tuning the absorption peak of the broad EPB to be on resonance with the excitation laser.[46] However, the majority of the particles are not excited at a particular excitation wavelength. The exact percentage of aggregates on resonance with a given excitation source is difficult to calculate without knowledge of the homogeneous line width of the individual aggregates. To date, we have not been able to determine the homogeneous line width; however, it is estimated that as few as 1% of the aggregates are on resonance with a particular excitation wavelength.[19] This parameter is important in estimating the SERS enhancement factor.

To perform the SERS experiments, the aggregate solution EPB maximum was tuned to 785 nm to maximize the number of aggregates on resonance with the excitation laser. It is assumed that the maximum of this band represents the average sized/shaped aggregates. At this excitation wavelength, 785 nm, Raman spectra were first taken without the addition of any analyte. This blank scan, shown in Figure 4, shows four strong peaks close to the Rayleigh line at 122, 162, 195, and 258 cm^{-1}. It is assumed that these bands are due to metal−sulfur or metal−chloride stretching modes from the adsorbed or chemisorbed

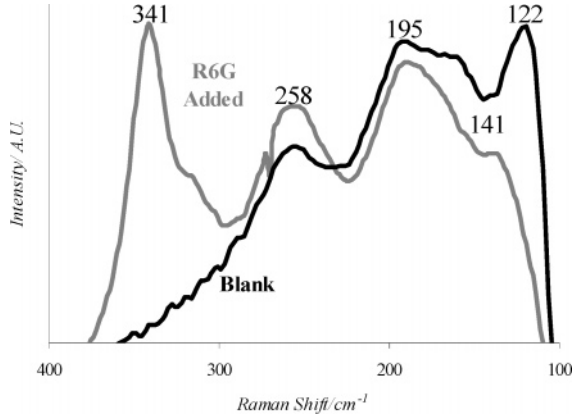

Figure 4. Low energy bands of GNAs alone (blank) and the shifted bands of GNAs with R6G added. The EPB has been tuned to be on resonance with 785 nm excitation.

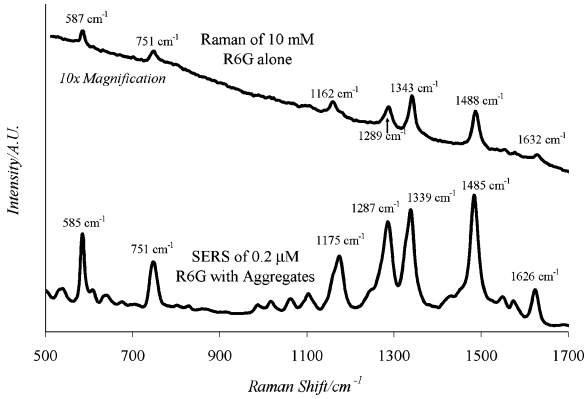

Figure 5. SERS spectrum of 0.2 μM R6G on gold nanoparticle aggregates and Raman spectrum of 10 mM R6G alone (magnified 10×) taken at the same excitation power and collection time. The EPB has been tuned to be on resonance with 785 nm excitation.

sulfur species and chloride ions on the surface; however, the complete assignment is prohibitively difficult at this time due to the complexity of the surface chemistry. Upon addition of any analyte molecule such as R6G, there is a substantial shift in these bands. This is apparent in the disappearance of the 122 cm^{-1} band and the appearance of the 341 cm^{-1} band. One possible explanation for this particular shift is the replacement of surface bound chloride with an analyte molecule. The 122 cm^{-1} peak is likely due to a gold−chloride vibrational mode.[52] If a surface bound analyte molecule such as R6G displaces the surface chloride, then the 122 cm^{-1} band will shift to a new frequency (e.g., the 341 cm^{-1} band), reflective of gold−analyte interaction. The exact nature of this mode is unclear at his point. Other low frequency modes are most likely due to gold−sulfur on the surface. Assuming analyte molecules bind to these surface sulfur species, one could possibly explain the small change in the SERS spectrum of R6G compared to its normal Raman spectrum by arguing that the direct interaction between R6G and the gold substrate is not strong.

By simple addition of R6G to the GNA solution, immediate and intense SERS signals were detected with 785 nm excitation (Figure 5). It is interesting to note that the SERS peaks from R6G are barely shifted, if at all, from the normal Raman peaks of R6G without enhancement. Usually, substantial changes in intensity and shifts in frequency in the SERS spectrum can be observed as compared to the normal Raman spectrum of a molecule due to interaction between the molecule and the SERS substrate. The insignificant spectral change observed here may be due to weak interaction between R6G and the SERS substrate. This observation is similar to previous SERS results of R6G on silver substrates.[53] Few studies have shown SERS of R6G from gold substrates because R6G usually does not strongly interact with gold surfaces.[54,55] In contrast, R6G readily adsorbs to silver and is detectable at nanomolar concentrations and below. The sensitivity of R6G detection by silver allowed the first SERS detection of single molecules.[21,56] Because gold substrates have historically been less sensitive to analytes such as R6G, they have been used less frequently. However, there are advantages of gold systems over silver. Silver is easily oxidized whereas gold is resistant to oxidation and is significantly more stable over time. In addition, gold aggregates can have absorption bands red shifted beyond those of silver, as far as 1 μm, providing more tunability and flexibility in the selection of excitation wavelengths. Core/shell structured substrates can provide similar tunability. However, core/shell structures have so far only exhibited low SERS enhancement factors, because they are not aggregated and lack the concentration of active surface sites of aggregates. In comparison, GNAs afford both tunability and large enhancement values, making aggregates attractive for molecular detection and structural analysis based on SERS. Gold nanoparticles made through the standard citrate reduction can be aggregated to show similar optical properties; however, the surface properties will be substantially different than the GNAs reported here.

The unique surface properties of these GNAs is one of their most important features.[55] Electron energy loss spectroscopy (EELS) has confirmed the presence of sulfur on the surface of the particles that appears to be effectively capping and linking the aggregates. EELS provides elemental, but not oxidation state, information about the surface sulfur. Therefore, the exact oxidation state and molecular form of these sulfur species are currently unknown and require further study in the future. However, preliminary near edge X-ray absorption fine structure (NEXAFS) measurements have shown that the sulfur species contain sulfur−oxygen bonds, possibly indicating sulfur oxides or simple sulfate ions.[49] The exact nature of these species is not yet known due to the difficulty of determining the chemical nature of species on the surface of nanomaterials. Regardless of their exact oxidation state or molecular form, however, the sulfur species are likely electron rich and are possibly strongly binding toward molecules such as R6G, which is positively charged, besides acting as the particle−particle "linker". In addition, the coverage of the surface sulfur species must be very thin, less than 4 nm, making the large SERS enhancements observed possible. The presence of sulfur species makes the surface of these nanoparticles and aggregates unique in comparison to other SERS substrates currently in use.[57]

To examine the viability of these GNAs as a general SERS substrate for a variety of applications, several biologically important molecules were tested including adenine, uridine, and several amino acids.[58−64] Upon the addition of aqueous solutions of these molecules, SERS signals were readily obtained with no further preparation (Figures 6 and 7). These spectra compare well with previously reported data as shown in Table 1. It is clear that many of the observed peaks were not previously observed in SERS studies. There are two possible explanations for this inconsistency. First, these experiments were all performed at the native pH of the GNA solutions without alteration (i.e., approximately pH 3). As most of the previous work was performed at near neutral pH, this could affect the spectra substantially, changing surface binding or protonation of the analyte molecules. As orientation on the surface and molecular

TABLE 1: Experimental (exp) and Literature (lit.) SERS Shifts of Various Biologically Relevent Molecules Detected with GNAs[a]

cysteine		histidine		lysine		adenine		uridine		tyrosine		methionine		leucine	
lit.[55]	exp	lit.[55, 56]	exp	lit.[55]	exp	lit.[54]	exp	lit.	exp	lit.[55]	exp	lit.[55]	exp	lit.[55]	exp
671	671		648	620	615	730	735		698	721	696	700	688	620	642
720	739	801	810		672	1339	1320		876	829	810	799	785	718	740
930	912	931	931	722	741	1482	1463		978		1053	874	874		1240
1067	1057		1008		868	1581	1564		1016	1199	1217		1033		1319
1140	1136	1160	1134	957	975				1244	1326	1303	1072	1066	1342	1362
1294	1294	1200	1191		1014				1396	1410	1402	1151	1145	1455	1468
1344	1346	1263	1252	1142	1134					1613	1593	1353	1350		
1411	1394	1312	1322		1242						1678		1390		
		1360	1363	1322	1327							1410	1417		
		1448	1463		1360										
		1571	1590	1410	1396										
				1464	1467										

[a] All positions in units of cm^{-1}.

structure change with pH, there can be significant changes in the SERS spectrum. Second, the surface of this GNA substrate is very different from any previously studied. The molecules may interact differently with this unique substrate, thereby changing the SERS spectra. In particular, because SERS spectra are dependent on molecular surface orientation, this interaction could have a substantial effect on the observed spectra. A comprehensive discussion of binding orientation and mechanism is beyond the scope of this paper.

Although not the first SERS detection of these compounds with the possible exception of uridine, this is their first observation utilizing gold SERS substrates. As mentioned earlier, gold substrates have many advantages over silver; however, until now surface chemistry has hindered its use. With an enhanced SERS-active surface, these GNAs have a distinct advantage over other gold SERS substrates. To provide a semiquantitative comparison, we will give a rough estimate of the SERS enhancement factor in the current study. By comparison of the intensities of the 1500 cm^{-1} peak of the Raman spectra of 10 mM R6G alone and 0.2 μM R6G in the presence of the aggregates, and including concentration differences, we obtain a 10^7 enhancement of the Raman signal (Figure 5). This enhancement factor is excellent for ensemble averaged, nonresonance SERS in comparison to previous enhancement factors.[65] If we assume that only about 1% of the aggregates are actually on resonance with the excitation wavelength, then the number of R6G molecules involved is reduced by a factor of about 100. Approximately 99% of the aggregates with R6G on their surface are not excited and thereby do not contribute to the SERS signal. Taking this factor into account, the enhancement would increase to about 10^9, which is one of the largest ensemble average enhancement factors reported for SERS substrates.[24,65,66]

There are two possible reasons for these large enhancements. First, the aggregates have an increased number of SERS active sites due to the great number of nanoparticle junctions present. Because R6G concentration is greater than one molecule per particle in this study, it is possible to have more than one molecule per aggregated enhanced. This also increases the probability for the analyte molecule to adsorb onto an enhancement site or hot spot as opposed to an adsorption site that has no enhanced EM field. Second, the unique surface properties of the GNAs facilitate efficient adsorption or binding of the analyte molecules onto the GNA surface.

To independently confirm the SERS activity of the GNAs, we have measured the SERS spectra of R6G on single GNAs using a different experimental setup in a different lab. With a

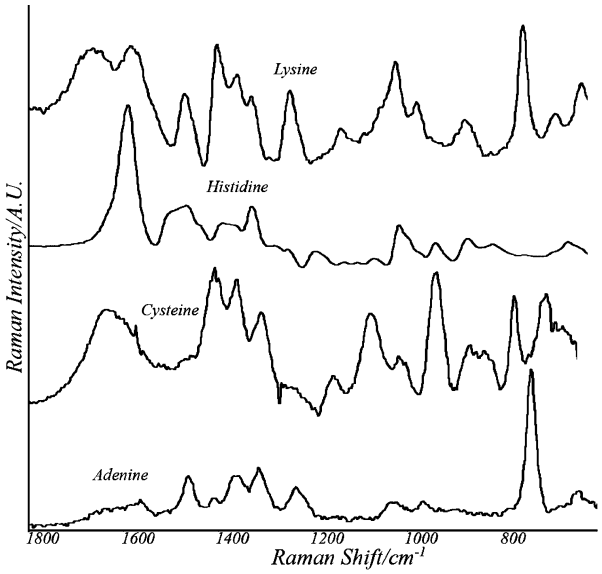

Figure 6. SERS spectra of adenine, cysteine, lysine, and histidine in the presence of gold nanoparticle aggregates at pH 3. The EPB has been tuned to be on resonance with 785 nm excitation.

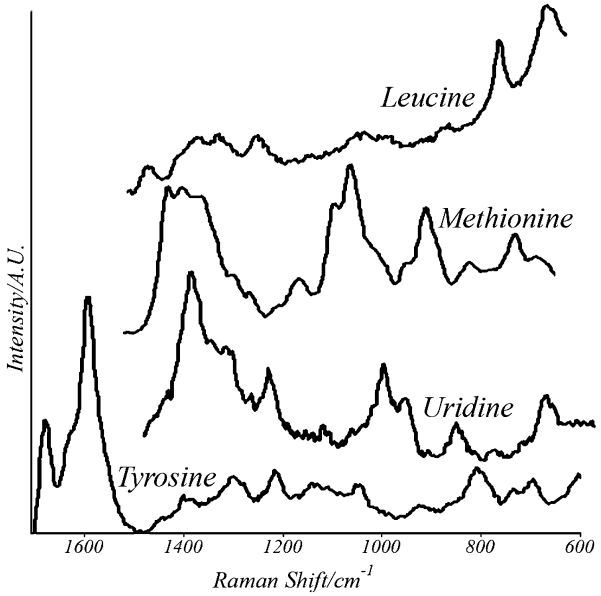

Figure 7. SERS spectra of tyrosine, uridine, methionine, and leucine in the presence of gold nanoparticle aggregates at pH 3. The EPB has been tuned to be on resonance with 785 nm excitation.

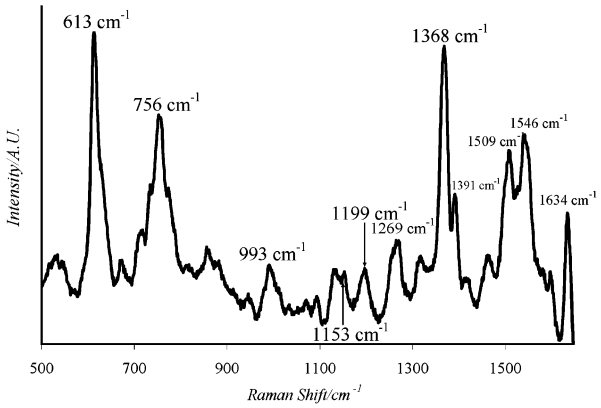

Figure 8. Representative single particle SERS spectrum of R6G on single gold nanoparticle aggregates immobilized to glass coverslips. The EPB of the GNA solution was tuned to maximize the number of resonant particles with excitation at 633 nm.

confocal micro-Raman setup, we are able to measure the SERS spectra of individual GNAs. Before application of any analyte solution to the sample slides, blank spectra were taken with no Raman signal observed for any of the examined single GNAs. Upon addition of a solution of R6G to the surface of the sample slide, a signal was immediately detected from a large number of individual GNAs (Figure 8). It is apparent that the single aggregate SERS signal is substantially different from that of the bulk system. This is not uncommon, and similar observations have been made in single silver aggregate studies.[19,67] This spectral change is due in part to the use of aggregated substrates. The surface of each aggregate is different, and therefore the surface location of each enhanced molecule varies. This could change the orientation of the molecule with respect to the active site, for example, in a junction or a dislocation in the surface. Because SERS is relative to the molecule's surface orientation, each aggregate can have a slightly different SERS signal; however, the bulk solution will average to the expected spectrum observed in Figure 5. Molecules were able to adsorb onto the aggregates in film form to yield strong SERS signals. This is encouraging particularly for applications requiring SERS measured in solid films. One important feature of a practical SERS sensor or detection device would be reusability of the substrate. This is only possible if the molecules detected can be readily removed so the GNA substrate can be reused. This was tested by removing the R6G by rinsing the substrate with water, at which point no SERS spectra were observed. With a fresh drop of R6G applied to the GNA substrate, equally strong SERS signals can be measured again. Therefore, the films of these GNAs are not only stable as mentioned earlier but also reusable, a very useful trait for many potential SERS applications.

Conclusion

A unique gold aggregate system has been shown experimentally to be useful for SERS detection of R6G and several biological molecules. R6G, a common molecule for SERS studies that is generally difficult to detect on gold substrates, readily adsorbs to these GNAs. This is believed to be due to the presence of sulfur species on the particle surface that provide strong binding of molecules of interest to the GNA. The SERS activity demonstrated for adenine, cysteine, lysine, histidine, leucine, methionine, uridine, and tyrosine shows the potential of the GNAs as convenient SERS substrates for biological and chemical sensing and analysis. On the basis of the surface properties of these GNAs, a wide variety of molecules can be detected via this unique SERS substrate that has been shown to be active for many molecules never before detected on gold substrates. These GNAs were shown to yield a large SERS enhancement of 10^7-10^9 for R6G. The large enhancement is partly attributed to aggregation that has been shown to substantially increase SERS signals. The potential of SERS using GNA films was tested based on single aggregate studies. It was found that R6G was immediately detectable with individual single aggregates immobilized onto glass slides, and the substrate appears to be reusable.

Acknowledgment. We acknowledge financial support of this project by the Petroleum Research Fund administered by the American Chemical Society (J.Z.Z.), the SEGRF Fellowship of Lawrence Livermore National Labs (LLNL) (A.M.S.), University of California Santa Cruz Faculty Research Fund (J.Z.Z.), and the Campus (UC)−Lab (LLNL) Exchange Program of the University of California Office of the President (J.Z.Z.). Work at LLNL was performed under the auspices of the U.S. Department of Energy by the University of California, Lawrence Livermore National Laboratory under Contract No. W-7405-Eng-48.

References and Notes

(1) Fleischman, M.; Hendra, P. J.; McQuillan, A. J. *Chem. Phys. Lett.* **1974**, *26*, 123.
(2) Albrecht, M. G.; Creighton, J. A. *J. Am. Chem. Soc.* **1977**, *99*, 5215.
(3) Jeanmaire, D. L.; Vanduyne, R. P. *J. Electroanal. Chem.* **1977**, *84*, 1.
(4) Grasselli, J. G.; Bulkin, B. J. *Analytical Raman Spectroscopy*; Wiley: New York, 1991.
(5) Schrader, B.; Bougeard, D. *Infrared and Raman Spectroscopy: Methods and Applications*; VCH: Weinheim; New York, 1995.
(6) Ferraro, J. R.; Nakamoto, K. *Introductory Raman Spectroscopy*; Academic Press: Boston, 1994.
(7) Shafer-Peltier, K. E.; Haynes, C. L.; Glucksberg, M. R.; Van Duyne, R. P. *J. Am. Chem. Soc.* **2003**, *125*, 588.
(8) Yonzon, C. R.; Haynes, C. L.; Zhang, X. Y.; Walsh, J. T.; Van Duyne, R. P. *Anal. Chem.* **2004**, *76*, 78.
(9) Sagmuller, B.; Schwarze, B.; Brehm, G.; Trachta, G.; Schneider, S. *J. Mol. Struct.* **2003**, *661*, 279.
(10) Taranenko, N.; Alarie, J. P.; Stokes, D. L.; VoDinh, T. *J. Raman Spectrosc.* **1996**, *27*, 379.
(11) Kneipp, K.; Haka, A. S.; Kneipp, H.; Badizadegan, K.; Yoshizawa, N.; Boone, C.; Shafer-Peltier, K. E.; Motz, J. T.; Dasari, R. R.; Feld, M. S. *Appl. Spectrosc.* **2002**, *56*, 150.
(12) Quinten, M. *Appl. Phys. B* **2000**, 70, 579.
(13) Zeman, E. J.; Schatz, G. C. *J. Phys. Chem.* **1987**, *91*, 634.
(14) Schatz, G. C.; VanDuyne, R. P. In *Handbook of Vibrational Spectroscopy*; Chalmers, J. M., Griffiths, P. R., Eds.; John Wiley and Sons: Chichester, U.K., 2002; Vol. 1; p 759.
(15) Otto, A.; Mrozek, I.; Grabhorn, H.; Akemann, W. *J. Phys.: Condens. Matter* **1992**, *4*, 1143.
(16) Moskovits, M. *Rev. Mod. Phys.* **1985**, *57*, 783.
(17) Kneipp, K.; Kneipp, H.; Itzkan, I.; Dasari, R. R.; Feld, M. S. *J. Phys.: Condens. Matter* **2002**, *14*, R597.
(18) Campion, A.; Kambhampati, P. *Chem. Soc. Rev.* **1998**, *27*, 241.
(19) Michaels, A. M.; Jiang, J.; Brus, L. *J. Phys. Chem. B* **2000**, *104*, 11965.
(20) Xu, H. X.; Bjerneld, E. J.; Kall, M.; Borjesson, L. *Phys. Rev. Lett.* **1999**, *83*, 4357.
(21) Kneipp, K.; Wang, Y.; Kneipp, H.; Perelman, L. T.; Itzkan, I.; Dasari, R.; Feld, M. S. *Phys. Rev. Lett.* **1997**, *78*, 1667.
(22) Blatchford, C. G.; Campbell, J. R.; Creighton, J. A. *Surf. Sci.* **1982**, *120*, 435.
(23) Brus, L. *Abstracts of Papers of the American Chemical Society* **2001**, *221*, 112.
(24) Nikoobakht, B.; El-Sayed, M. A. *J. Phys. Chem. A* **2003**, *107*, 3372.
(25) Creighton, J. A. Metal Colloids. In *Surface Enhanced Raman Scattering*; Chang, R. K., Furtak, T. E., Eds.; Plenum Press: New York and London, 1982; p 315.
(26) Faulds, K.; Littleford, R. E.; Graham, D.; Dent, G.; Smith, W. E. *Anal. Chem.* **2004**, *76*, 592.
(27) Kneipp, K.; Kneipp, H.; Manoharan, R.; Hanlon, E. B.; Itzkan, I.; Dasari, R. R.; Feld, M. S. *Appl. Spectrosc.* **1998**, *52*, 1493.
(28) Shipway, A. N.; Lahav, M.; Gabai, R.; Willner, I. *Langmuir* **2000**, *16*, 8789.

(29) Nikoobakht, B.; El-Sayed, M. A. *Chem. Mater.* **2003**, *15*, 1957.
(30) Prodan, E.; Nordlander, P.; Halas, N. J. *Nano Lett.* **2003**, *3*, 1411.
(31) Quinten, M. *J. Cluster Sci.* **1999**, *10*, 319.
(32) Quinten, M. *Appl. Phys. B* **2001**, 73, 245.
(33) Martin, O. J. F. Plasmon Resonances in Nanowires with a Nonregular Cross Section. In *Optical Nanotechnologies: The Manipulation of Surface and Local Plasmons*; Tominaga, J., Tsai, D. P., Eds.; Springer: Berlin, New York, 2003; p 183.
(34) Jin, R. C.; Cao, Y. W.; Mirkin, C. A.; Kelly, K. L.; Schatz, G. C.; Zheng, J. G. *Science* **2001**, *294*, 1901.
(35) Kottmann, J. P.; Martin, O. J. F.; Smith, D. R.; Schultz, S. *Opt. Express* **2000**, *6*, 213.
(36) Maillard, M.; Giorgio, S.; Pileni, M. P. *J. Phys. Chem. B* **2003**, *107*, 2466.
(37) Quinten, M.; Kreibig, U. *Appl. Opt.* **1993**, *32*, 6173.
(38) Tao, A.; Kim, F.; Hess, C.; Goldberger, J.; He, R. R.; Sun, Y. G.; Xia, Y. N.; Yang, P. D. *Nano Lett.* **2003**, *3*, 1229.
(39) Oldenburg, S. J.; Westcott, S. L.; Averitt, R. D.; Halas, N. J. *J. Chem. Phys.* **1999**, *111*, 4729.
(40) Doering, W. E.; Nie, S. M. *Anal. Chem.* **2003**, *75*, 6171.
(41) Jana, N. R. *Analyst* **2003**, *128*, 954.
(42) Jackson, J. B.; Westcott, S. L.; Hirsch, L. R.; West, J. L.; Halas, N. J. *Appl. Phys. Lett.* **2003**, *82*, 257.
(43) Grant, C. D.; Schwartzberg, A. M.; Norman, T. J.; Zhang, J. Z. *J. Am. Chem. Soc.* **2003**, *125*, 549.
(44) Schwartzberg, A. M.; Grant, C.; Wolcott, A.; Zhang, J. Z.; Talley, C. E. *Proc. SPIE—Int. Soc. Opt. Eng.*, **2003**.
(45) Norman, T. J.; Grant, C. D.; Magana, D.; Zhang, J. Z.; Liu, J.; Cao, D. L.; Bridges, F.; Van Buuren, A. *J. Phys. Chem. B* **2002**, *106*, 7005.
(46) Schwartzberg, A. M., Grant, C. D., Wolcott, A., Bogomolni, R., and Zhang, J. Z. *Proc. SPIE—Int. Soc. Opt. Eng.* **2003**, *5221*, To Be Released.
(47) Norman, T. J.; Grant, C. G.; Schwartzberg, A. M.; Zhang, J. Z. *Phys. Rev. B* Submitted.
(48) Creighton, J. A.; Blatchford, C. G.; Albrecht, M. G. *J. Chem. Soc., Faraday Trans. 2* **1979**, *75*, 790.
(49) Norman, T. J.; Grant, C.; Magana, D.; Anderson, R.; Zhang, J. Z.; Cao, D.; Bridges, F.; Liu, J.; Van Buuren, A. *Proc. SPIE—Int. Soc. Opt. Eng.* **2002**, *4807*, 51.
(50) Quinten, M.; Schonauer, D.; Kreibig, U. *Z. Phys. D: At., Mol. Clusters* **1989**, *12*, 521.
(51) Schonauer, D.; Quinten, M.; Kreibig, U. *Z. Phys. D: At., Mol. Clusters* **1989**, *12*, 527.
(52) Cotton, F. A. *Advanced Inorganic Chemistry*; Interscience Publishers: New York, 1962.
(53) Hildebrandt, P.; Stockburger, M. *J. Phys. Chem.* **1984**, *88*, 5935.
(54) Gupta, R.; Weimer, W. A. *Chem. Phys. Lett.* **2003**, *374*, 302.
(55) Maya, L.; Vallet, C. E.; Lee, Y. H. *J. Vac. Sci. Technol., A* **1997**, 15, 238.
(56) Nie, S. M.; Emery, S. R. *Science* **1997**, *275*, 1102.
(57) Doering, W. E.; Nie, S. M. *J. Phys. Chem. B* **2002**, *106*, 311.
(58) Perno, J. R.; Grygon, C. A.; Spiro, T. G. *J. Phys. Chem.* **1989**, *93*, 5672.
(59) Stewart, S.; Fredericks, P. M. *Spectrochim. Acta, Part A* **1999**, 55, 1641.
(60) Martusevicius, S.; Niaura, G.; Talaikyte, Z.; Razumas, V. *Vib. Spectrosc.* **1996**, *10*, 271.
(61) Kim, S. K.; Kim, M. S.; Suh, S. W. *J. Raman Spectrosc.* **1987**, *18*, 171.
(62) Chumanov, G. D.; Efremov, R. G.; Nabiev, I. R. *J. Raman Spectrosc.* **1990**, *21*, 43.
(63) Nabiev, I. R.; Chumanov, G. D.; Efremov, R. G. *J. Raman Spectrosc.* **1990**, *21*, 49.
(64) Lee, H.; Kim, M. S.; Suh, S. W. *J. Raman Spectrosc.* **1991**, *22*, 91.
(65) Kneipp, K.; Kneipp, H.; Itzkan, I.; Dasari, R. R.; Feld, M. S. *Chem. Rev.* **1999**, *99*, 2957.
(66) GarciaVidal, F. J.; Pendry, J. B. *Phys. Rev. Lett.* **1996**, *77*, 1163.
(67) Michaels, A. M.; Nirmal, M.; Brus, L. E. *J. Am. Chem. Soc.* **1999**, *121*, 9932.